Journal of Magnetism and Magnetic Materials 471 (2019) 110–115

Contents lists available at ScienceDirect

Journal of Magnetism and Magnetic Materials

journal homepage: www.elsevier.com/locate/jmmm

Research articles

Improvement of soft magnetic properties for distinctly high Fe content amorphous alloys via longitudinal magnetic field annealing

Hu Li[a,b], Aina He[b,c], Anding Wang[b,c,*], Lei Xie[a,b], Qiang Li[a,*], Chengliang Zhao[b,c], Guoyang Zhang[b], Pingbo Chen[b]

[a] School of Physics Science and Technology, Xinjiang University, Ürümqi 830046, Xinjiang, China
[b] Key Laboratory of Magnetic Materials and Devices, Ningbo Institute of Materials Technology and Engineering, Chinese Academy of Sciences, Ningbo 315201, Zhejiang, China
[c] Zhejiang Province Key Laboratory of Magnetic Materials and Application Technology, Ningbo Institute of Materials Technology and Engineering, Chinese Academy of Sciences, Ningbo 315201, China

ARTICLE INFO

Keywords:
Amorphous alloy
Magnetic field annealing
Soft-magnetic properties
Magnetic domain

ABSTRACT

The effects of longitudinal magnetic field annealing on soft-magnetic properties (SMPs) and magnetic domain structure of $Fe_{(82.6\text{-}85.7)}Si_{(2\text{-}4.9)}B_{(9.2\text{-}11.2)}P_{(1.5\text{-}2.7)}C_{0.8}$ amorphous alloys with a distinctly high Fe content of 93.5–95.5 wt% for high B_s were investigated. It was found that longitudinal magnetic field annealing could improve soft-magnetic properties (SMPs) of amorphous alloys effectively, except the one with poor thermal stability. Superb magnetic properties containing a minimum coercivity of 0.8 A/m, a maximum effective permeability of 11×10^3 at 1 kHz and minimum core loss of 0.052 W/kg (at $B_m = 0.9$ T and $f = 50$ Hz) were successfully obtained. Domain structures were characterized with a Magneto-optical Kerr Microscope to unveil the mechanism of SMPs improvement. Stripe domains were observed in the annealed high Fe content amorphous alloy ribbons with optimal soft magnetic properties.

1. Introduction

Fe-based amorphous alloys have aroused worldwide interests from both scientific and technologic aspects due to their excellent soft-magnetic properties (SMPs) [1,2], and energy saving effect [3]. Further improvements of their] magnetic properties and formability are long-term hot spots, which promote new alloy design theories and preparation techniques [4,5]. The relatively lower saturation magnetic flux density (B_s) determined by Fe content that compared with silicon steels is the most notable shortcoming and inhabit their wider application [6,7]. Breaking though the Fe content limitation and developing high Fe content amorphous alloys are quite desired, but are difficult. The reported high Fe content alloys have suffered the poor formability and deteriorated soft magnetic properties [8,9]. In our previous work [10], $Fe_{(82.6\text{-}85.7)}Si_{(2\text{-}4.9)}B_{(9.2\text{-}11.2)}P_{(1.5\text{-}2.7)}C_{0.8}$ amorphous alloys with a distinctly high Fe content and good manufacturability were successfully developed, which exhibit attractive application prospects if the softness can be improved. Many researchers recently studied the effects of magnetic field annealing on softness of amorphous and nanocrystalline alloys [9,11–13]. Suzuki et al. [12], investigated the influence of magnetic field annealing on crystal magnetic anisotropy in nanocrystalline soft-magnetic alloys, and found that SMPs could be improved effectively. Zhao et al. [13], studied the effect of longitudinal field annealing on Fe(Co)-based amorphous alloys, and found that SMPs could be improved for the alloys with high Curie temperature (T_c). These studies indicated that magnetic field annealing could promote inner stress release and modulate the domain structure which directly affects the soft-magnetic alloys [12,14,15]. However, for the $Fe_{(82.6\text{-}85.7)}Si_{(2\text{-}4.9)}B_{(9.2\text{-}11.2)}P_{(1.5\text{-}2.7)}C_{0.8}$ amorphous alloys with a distinctly high Fe content, the annealing process not only leads to structure relaxation and stress release [13,16], but also clustering [13,17–19]. The correlation between magnetic field annealing temperature and SMPs needs further investigation, which have great importance on understanding the structure evolution processes.

In this study, the effects of longitudinal magnetic field annealing on SMPs of these high Fe content amorphous alloys were investigated. In order to reveal the correlation between drastically improved SMPs and magnetic structure, magnetic domains were also studied.

* Corresponding authors at: Key Laboratory of Magnetic Materials and Devices, Ningbo Institute of Materials Technology and Engineering, Chinese Academy of Sciences, Ningbo 315201, Zhejiang, China (A. Wang).
E-mail addresses: anding@nimte.ac.cn (A. Wang), qli@xju.edu.cn (Q. Li).

https://doi.org/10.1016/j.jmmm.2018.09.072
Received 1 June 2018; Received in revised form 1 August 2018; Accepted 20 September 2018
Available online 21 September 2018
0304-8853/

2. Experimental procedures

Amorphous alloy ribbons with nominal compositions (at.%) of $Fe_{82.7}Si_{4.9}B_{9.2}P_{2.4}C_{0.8}$, $Fe_{82.6}Si_{3.7}B_{10.9}P_2C_{0.8}$, $Fe_{83.3}Si_2B_{11.2}P_{2.7}C_{0.8}$, $Fe_{84.2}Si_{2.1}B_{11}P_{1.9}C_{0.8}$, and $Fe_{85.7}Si_{2.3}B_{9.7}P_{1.5}C_{0.8}$ were prepared by a single Cu roller melt-spinning technique. The ribbon with a width of about 1 mm and a thickness of approximately 25 µm, was cut into 50 mm length for annealing and measurements. The amorphous structure of the as-quenched samples was confirmed by X-ray diffraction (XRD) with Cu Kα radiation. Before measuring the magnetic properties, the ribbon samples were annealed at 280–420 °C for 15 min in a vacuum quartz tube with a magnetic field of 1.6×10^3 A/m applied along longitudinal direction (the ribbon axis). The coercivity (H_c) was measured by a DC B-H hysteresis loop tracer under a field of 800 A/m. The measurements of core losses (P) and AC hysteresis loops were carried out by utilizing AC B-H loop tracer under different frequencies of 50, 200 and 1000 Hz, respectively. Permeability (μ_e) at the field of 1 A/m was measured by an impedance analyzer at a frequency range from 1 kHz to 10 MHz. The saturation magnetic flux density (B_s) was tested with a vibrating sample magnetometer (VSM) under a maximum applied field of 800 kA/m. Magnetic domain structure of the ribbon samples was observed by using a Magneto-optical Kerr Microscope. All the measurements were carried out at room temperature.

3. Results and discussion

Fig. 1(a) shows the variation of H_c as a function of annealing temperature (T_A). All the alloys exhibit a similar tendency, i.e., H_c first decreases to a minimum at a T_A (henceforth referred as optimal T_A) and then increases drastically with increasing T_A from 280 °C to 420 °C. The decreases of H_c below optimal T_A can be attributed to the inner stress release during structural relaxation [20]. Besides, the co-effects of magnetic and thermal fields promote the micro-structure uniformity [9,11], thus improve their SMPs. The increase of H_c over optimal T_A may be ascribed to partial crystallization or clustering, which deteriorate the SMPs due to the formation of hard magnetic phase such as boride and heterogeneous micro-structure with some overgrowth α-Fe grains. Fig. 1(b) displays the different performance of H_c for $Fe_{(82.6\text{-}85.7)}Si_{(2\text{-}4.9)}B_{(9.2\text{-}11.2)}P_{(1.5\text{-}2.7)}C_{0.8}$ alloys treated by longitudinal magnetic field annealing (FA) and normal annealing (NA) without magnetic field application, after annealing at optimal T_A. The H_c of the alloys treated by NA were reported before [10], which were annealed by using the same furnace. It is clear that the FA can effectively improve the H_c of $Fe_{82.7}Si_{4.9}B_{9.2}P_{2.4}C_{0.8}$, $Fe_{82.6}Si_{3.7}B_{10.9}P_2C_{0.8}$, $Fe_{83.3}Si_2B_{11.2}P_{2.7}C_{0.8}$ and $Fe_{84.2}Si_{2.1}B_{11}P_{1.9}C_{0.8}$ alloys. However, for the $Fe_{85.7}Si_{2.3}B_{9.7}P_{1.5}C_{0.8}$ amorphous alloy with highest Fe content, H_c increases from 5.9 A/m for the NA sample to 14.7 A/m for the FA sample. It is hence concluded that the FA is not universally effective for all amorphous alloys.

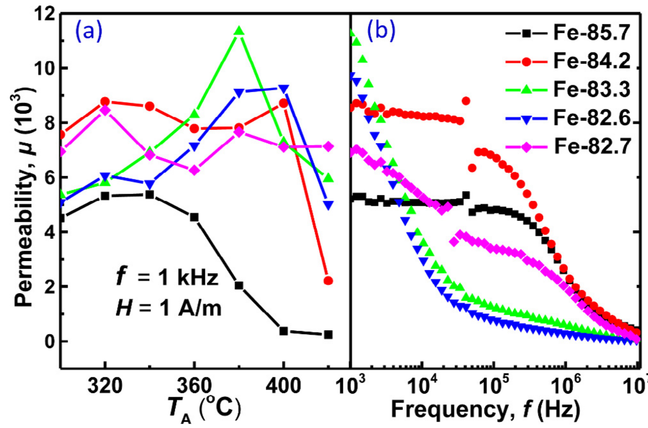

Fig. 2. (a) The dependence of effective permeability (μ_e) on T_A at a frequency (f) of 1 kHz and 1 A/m for $Fe_{(82.6\text{-}85.7)}Si_{(2\text{-}4.9)}B_{(9.2\text{-}11.2)}P_{(1.5\text{-}2.7)}C_{0.8}$ amorphous alloys. (b) The dependence of effective permeability (μ_e) on f of samples treated by longitudinal FA at 380 °C for 15 min.

As we know, μ_e is another important parameters of soft-magnetic materials, thus we also studied the influence of FA on μ_e of $Fe_{(82.6\text{-}85.7)}Si_{(2\text{-}4.9)}B_{(9.2\text{-}11.2)}P_{(1.5\text{-}2.7)}C_{0.8}$ amorphous alloys. As shown in Fig. 2(a), the μ_e at 1 kHz of the present high Fe content amorphous alloys annealed by FA first increases and then decreases as the T_A increases, and the trend of μ_e with T_A is opposite to that of H_c, as shown in Fig. 1(a). Compared with the results of NA samples [3], the μ_e is obviously improved by the method of FA. For these alloys with improved soft magnetic properties, the optimal μ_e are of quite high values of 7.8–11 $\times 10^3$, which are even better than that of the commercial FeSiB and FeSiBC alloys [21,22]. Fig. 2(b) shows the μ_e of the samples annealed at optimal T_A as a function of frequency. It is clear that the change tendencies are quite different, i.e., the $Fe_{82.6}Si_{3.7}B_{10.9}P_2C_{0.8}$ and $Fe_{83.3}Si_2B_{11.2}P_{2.7}C_{0.8}$ alloys exhibit highest μ_e at low f of about 1 kHz and drastically decreased μ_e at high f, the $Fe_{84.2}Si_{2.1}B_{11}P_{1.9}C_{0.8}$ alloy exhibit attractively high and constant μ_e in large f range of 1–20 kHz. It is hence concluded that the alloys with FA annealing can has wide application fields.

As shown in Fig. 3(a), the change of core loss with T_A shows a similar trend to H_c for the present amorphous alloys. All alloys exhibit minimum core loss of 0.052–0.1 W/kg at T_A of 380–400 °C and at a frequency of 50 Hz and an induction (B_m) of 0.9 T. It should be noted that the optimal core loss of the annealed $Fe_{85.7}Si_{2.3}B_{9.7}P_{1.5}C_{0.8}$ alloy is relatively larger than other alloys mentioned above, and thus the results

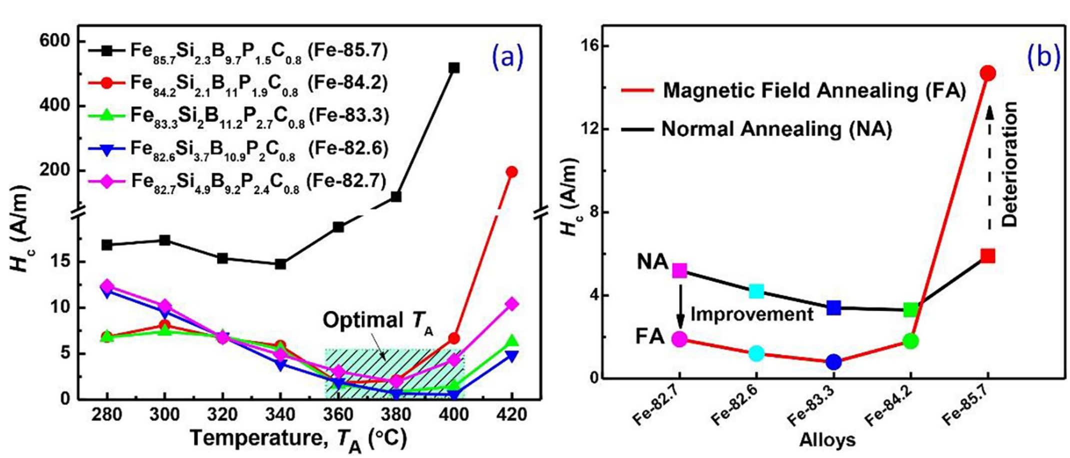

Fig. 1. . (a) The dependence of H_c on T_A of $Fe_{(82.6\text{-}85.7)}Si_{(2\text{-}4.9)}B_{(9.2\text{-}11.2)}P_{(1.5\text{-}2.7)}C_{0.8}$ amorphous alloys treated by longitudinal magnetic field annealing (FA) with an applied field of 1.6×10^3 A/m and (b) the difference of H_c for FA and normal field-free annealing (NA) at the optimal T_A.

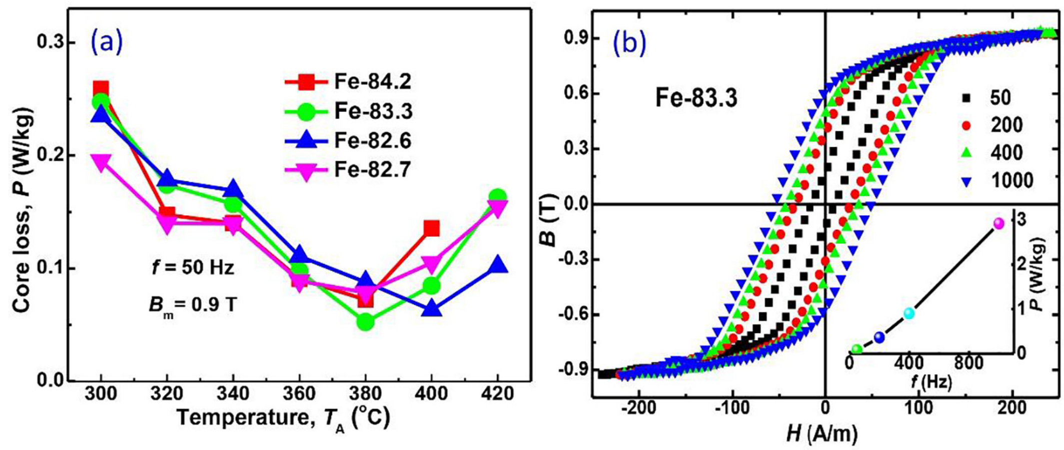

Fig. 3. (a) Core loss as a function of T_A for $Fe_{(82.6\text{-}84.2)}Si_{(2\text{-}4.9)}B_{(9.2\text{-}11.2)}P_{(1.5\text{-}2.7)}C_{0.8}$ amorphous alloys treated by longitudinal FA, (b) the AC B-H hysteresis loops for the annealed $Fe_{83.3}Si_2B_{11.2}P_{2.7}C_{0.8}$ alloy measured at different frequencies (*f*).

of this alloy are not included in Fig. 3(a). The Fig. 3(b) shows the hysteresis loops measured at different *f* of 50, 200, 400 and 1 kHz for the $Fe_{83.3}Si_2B_{11.2}P_{2.7}C_{0.8}$ alloy annealed by FA at optimal T_A. As we can see, the area of hysteresis loop increase smoothly with *f* increases from 50 Hz to 1 kHz. The inset of Fig. 3(b) shows the dependence of core loss on *f*. The alloy exhibits extremely low core loss of 0.05–2.9 W/kg in the *f* range from 50 Hz to 1 kHz.

Fig. 4(a) illustrates the hysteresis loops of the $Fe_{(82.6\text{-}85.7)}Si_{(2\text{-}4.9)}B_{(9.2\text{-}11.2)}P_{(1.5\text{-}2.7)}C_{0.8}$ amorphous alloys measured with a VSM. As enlarged in inset (b), these high Fe content alloys exhibit B_s of 1.62–1.66 T. Compared with the results of NA [10], FA has slight effect on B_s of the present alloys. Since the B_s of the amorphous alloy is mainly depend on the composition and the microstructure of clusters [23], it is speculated that the FA does not affect the structural phase transition and atomic arrangement. Inset table gives a comparison of the magnetic properties of the present alloys with different annealing methods and that of the commercial alloys. It is clear that the high Fe content $Fe_{(82.6\text{-}85.7)}Si_{(2\text{-}4.9)}B_{(9.2\text{-}11.2)}P_{(1.5\text{-}2.7)}C_{0.8}$ alloys subjected to FA annealing exhibit superb soft magnetic properties. The longitudinal FA can effectively improve the soft magnetic properties of these amorphous alloys with distinctly high Fe content, which will promote the application.

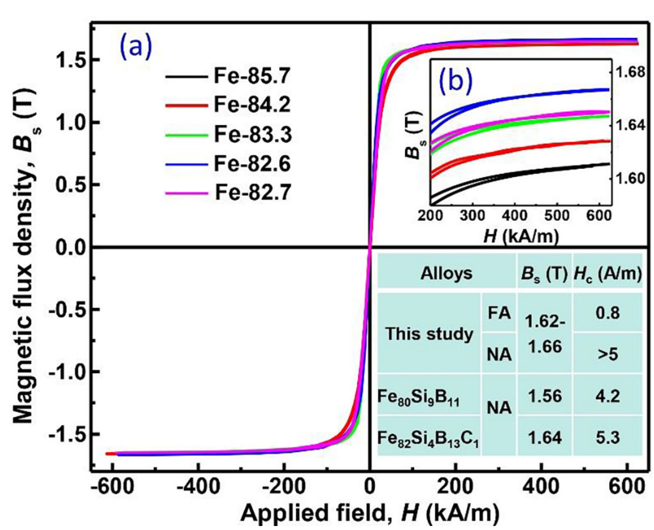

Fig. 4. . (a) Hysteresis loops for $Fe_{(82.6\text{-}85.7)}Si_{(2\text{-}4.9)}B_{(9.2\text{-}11.2)}P_{(1.5\text{-}2.7)}C_{0.8}$ amorphous alloys subjected to a longitudinal FA. (b) Inset of the partial amplified hysteresis loops. The insert table shows the B_s and H_c of the present alloys for a normal annealing (NA) and a magnetic field annealing (FA), as well as the commercial alloys.

To sum up, the longitudinal magnetic field annealing is effectively in improving the SMPs of amorphous alloys with distinctly high Fe content, except the $Fe_{85.7}Si_{2.3}B_{9.7}P_{1.5}C_{0.8}$ alloys with critical Fe content. Superb magnetic properties containing a minimum coercivity of 0.8 A/m, a maximum effective permeability of 11×10^3 at 1 kHz and minimum core loss of 0.052 W/kg (at $B_m = 0.9$ T and $f = 50$ Hz) were successfully obtained, which were much better than the commercial alloys. It is of great interests to understand the reasons for the improvement of the SMPs for the four alloys and also the deterioration of the alloy with critical Fe content.

First, we identify the magnetic domain structure changes of the two typical $Fe_{83.3}Si_2B_{11.2}P_{2.7}C_{0.8}$ and $Fe_{85.7}Si_{2.3}B_{9.7}P_{1.5}C_{0.8}$ amorphous alloys. As shown in Fig. 5(a) and (b), both the AQ and annealed ribbons of $Fe_{83.3}Si_2B_{11.2}P_{2.7}C_{0.8}$ alloy exhibit regular shape of stripe magnetic domains. Compared with the irregular branch magnetic domains in AQ sample, the stripe in the annealed sample is much more uniform showing no branches, indicating that the pinning center correlate to the stress and structural heterogeneities. This should be the reason why longitudinal FA can effectively improve the soft magnetic properties by accelerating the internal stress release and modulating the domain structure [11,12]. However, for the $Fe_{85.7}Si_{2.3}B_{9.7}P_{1.5}C_{0.8}$ alloy, irregular magnetic domains with small width are presented in both AQ and annealed samples, as shown in Fig. 6(c) and (d). Despite the width is more uniform, the domain pattern is occupied with high density of

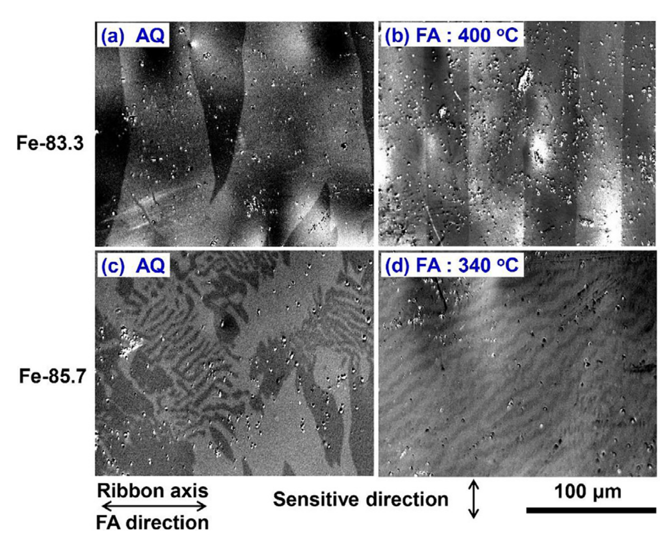

Fig. 5. Images of magnetic domain structures of $Fe_{83.3}Si_2B_{11.2}P_{2.7}C_{0.8}$ and $Fe_{85.7}Si_{2.3}B_{9.7}P_{1.5}C_{0.8}$ alloy ribbons with different states.

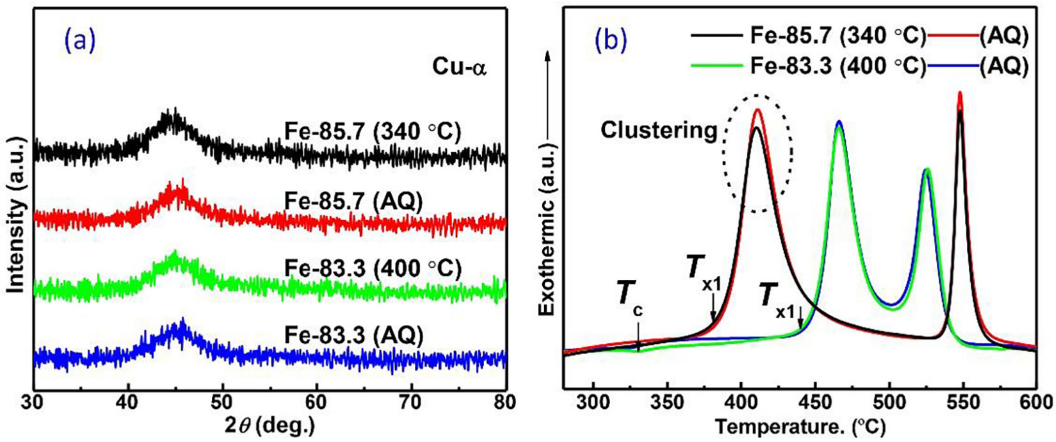

Fig. 6. (a) XRD patterns and (b) DSC curves of $Fe_{83.3}Si_2B_{11.2}P_{2.7}C_{0.8}$ and $Fe_{85.7}Si_{2.3}B_{9.7}P_{1.5}C_{0.8}$ alloy ribbons with different states.

branches, illustrating the strong pinning effect. The domain structure of the four samples are quite consistent with the former SMP changes.

Since the domain structure and soft magnetic properties were mainly depended on the microstructure containing amorphous structure as well as the precipitated phase during annealing [8,24], we then identified the multiscale change of structure, to reveal the origin of different magnetic performance. X-ray diffraction (XRD) and differential scanning calorimeter (DSC) were performed for the $Fe_{83.3}Si_2B_{11.2}P_{2.7}C_{0.8}$ and $Fe_{85.7}Si_{2.3}B_{9.7}P_{1.5}C_{0.8}$ alloys. As shown in Fig. 6(a), no sharp diffraction peaks of crystallization are detected, showing the amorphous structure in XRD resolution for all samples. According to the DSC curves of the four samples shown in the Fig. 6(b), obvious differences can be found for the two kinds of ribbon samples. The curves of the AQ and annealed $Fe_{83.3}Si_2B_{11.2}P_{2.7}C_{0.8}$ samples almost overlap each other. But for the $Fe_{85.7}Si_{2.3}B_{9.7}P_{1.5}C_{0.8}$ alloy ribbon annealed at 340 °C, the exothermic peak of the first initial crystallization peak is relatively lower than as-quenched one. This directly proves the drastic clustering of α-Fe which has been reported before [10,17]. It is well accepted that the good soft magnetic properties of the amorphous alloys are attribute to the uniform microstructure with eliminated free volume and without crystallization or clustering. The narrow temperature interval between the T_c and T_{x1} indicates the poor thermal stability of the $Fe_{85.7}Si_{2.3}B_{9.7}P_{1.5}C_{0.8}$ amorphous alloy, which cannot inhibit clustering or crystallization before thorough structure relaxation and stress release. It is noted that the Fe content of the $Fe_{85.7}Si_{2.3}B_{9.7}P_{1.5}C_{0.8}$ alloy is closed to the upper limit and critical amorphous forming ability, which means low amorphicity and high density of defects like free volume and clusters of the AQ sample [25]. This is the reason why the AQ sample of $Fe_{85.7}Si_{2.3}B_{9.7}P_{1.5}C_{0.8}$ alloy exhibit higher H_c. During the annealing process, the internal stress cannot be thoroughly released and more clusters will formed [17,26], leading to higher pinning effects and deteriorated soft magnetic properties of $Fe_{85.7}Si_{2.3}B_{9.7}P_{1.5}C_{0.8}$ alloy [27]. For other alloys with high thermal stability and large T_{x1}-T_c, the AQ samples are of high amorphicity and the structure will homogeneity during the annealing process. It is concluded that the good amorphicity and high thermal stability are essential for excellent soft magnetic properties, no matter what annealing methods are used.

At last, we proposed a schematic diagram of the domain structure changes during FA and NA, as shown in Fig. 7(d) and (e), to simplify the understanding of the improvement and deterioration of the soft magnetic properties. The applied field direction is along the axis of ribbon, as shown in Fig. 7(a). Fig. 7(b) shows the magnetic domain structure and the direction of atomic magnetic moments (μ_J) of the AQ samples. Generally, the variations of domain microstructures can be elucidated by classical Weiss molecular field theory [28]. According to this theory, the μ_J are parallel to each other in a domain due to the exchange interaction [29], but the alignment direction of μ_J varies from domain to domain. It has been reported that the Curie temperatures of the amorphous alloys (T_c-amor) and α-Fe cluster (T_c-clu) are different [30], as shown in Fig. 7(c). The T_c-amor is lower than the annealing temperature (T_A). The T_c-clu is higher than the T_c-amor and will increases with the cluster size and magnetic interaction. For the $Fe_{85.7}Si_{2.3}B_{9.7}P_{1.5}C_{0.8}$ alloy with low thermal stability, the cluster will grow and the T_c-clu will be higher than the T_A after annealing. Therefore, the isothermal annealing process will lead to the precipitation and growth of α-Fe clusters with high T_c-clu [17], which will influence the relaxation and inhibit the stress release of amorphous alloys, and leads to high magnetic anisotropy and bad soft magnetic properties [31]. During the isothermal annealing process, the alloys with high thermal stability are in paramagnetic state and the structure relaxation will perform freely, resulting in high homogeneity and low stress. In the NA cooling stage, the magnetic moments of cluster will return to ferromagnetic state early and preform magnetic domains, leading to induced anisotropy, which is the reason why the alloys with distinctly high Fe content exhibit comparatively worse soft magnetic properties. In the FA cooling stage, the magnetic moments of the cluster and the amorphous will be aligned to the easy magnetization direction by the applied magnetic field, resulting in the great improvement of soft magnetic properties. As studied by Severino [32] and Miguel [33] et al., in Co-based amorphous, the FA treatment substantially increases longitudinal anisotropy and improves the SMPs as it is expected. The magnetization process in longitudinal direction is mainly caused by a displacement of the domain walls. It has also been reported that a large longitudinal anisotropy can increase the magnetic-resonance frequency, which is advantageous for the good permeability-frequency (μ-f) property in the high-frequency region, amplifying the advantage of amorphous alloy in devices with fixed magnetic path like transformer, induction and etc. In a different sense, though, the large anisotropy will lead to rotation of domain walls during magnetization and deteriorated SMPs in the transverse direction. It is hence concluded that the FA treated amorphous alloys are not good for applications in electric motor and other devices with alternating magnetic fields.

It should be noted that magnetostriction (λ_s) is also affected by FA and has a critical influence on SMPs. During the annealing of an amorphous alloy, structural relaxation occurs and is accompanied to various degrees by a change in magnetostriction. Ho et al. has proposed that the changes of magnetostriction for Fe-based, FeNi-based and Co-based amorphous alloys are quite different [34]. The influence of FA on the SMPs of the high Fe content amorphous alloys with poor thermal stability should be more complicated and need more investigations.

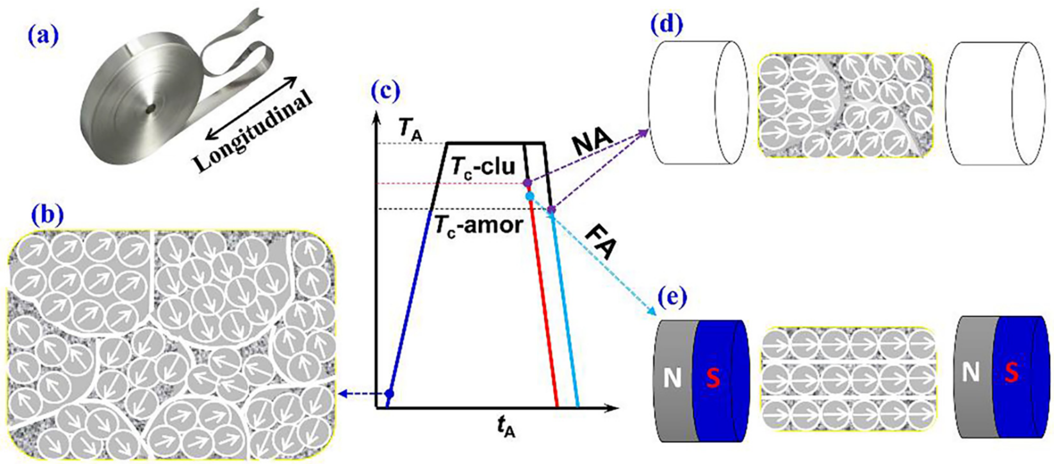

Fig. 7. (a) Applied field direction along the ribbon axial; (b) A sketch of magnetic domain structures of as-quenched ribbon; (c) Magnetic state of the amorphous alloys and clusters in the annealing process; (d) and (e) are the variation of magnetic moment and domain structure for the annealed ribbon by a normal field-free annealing (NA) and a longitudinal magnetic field annealing (FA), respectively.

4. Conclusions

The effects of longitudinal magnetic field annealing on SMPs of $Fe_{(82.6\text{-}85.7)}Si_{(2\text{-}4.9)}B_{(9.2\text{-}11.2)}P_{(1.5\text{-}2.7)}C_{0.8}$ amorphous alloys with high Fe content have been investigated and the conclusions are summarized as follows:

1. For the high thermal stability amorphous alloys, longitudinal magnetic field annealing can improve SMPs effectively.
2. Excellent magnetic properties containing a minimum coercivity of 0.8 A/m, a maximum effective permeability of 11×10^3 at 1 kHz and minimum core loss of 0.052 W/kg (at $B_m = 0.9$ T and $f = 50$ Hz) were successfully obtained.
3. Magnetic domain structure correlates to SMPs of amorphous alloys closely. Stripe domain which shows more uniformity at optimal T_A exhibits excellent SMPs.
4. The magnetic moment of the cluster and the amorphous will be aligned to the easy magnetization direction by the applied longitudinal magnetic field annealing, resulting in the great improvement of soft magnetic properties.

Acknowledgements

This work was supported by the National Key Research and Development Program of China (2017YFB0903902), the National Natural Science Foundation of China (Grant No. 51601206, 51771159, 51771083), and the Zhejiang Provincial Natural Science Foundation (LQ18E010006).

Appendix A. Supplementary data

Supplementary data to this article can be found online at https://doi.org/10.1016/j.jmmm.2018.09.072.

References

[1] A.D. Wang, C.L. Zhao, A.N. He, H. Men, C.C. Chang, X.M. Wang, Composition design of high B_s Fe-based amorphous alloys with good amorphous-forming ability, J. Alloy. Compd. 656 (2016) 729–734.
[2] W.J. Yuan, F.J. Liu, S.J. Pang, Y.J. Song, T. Zhang, Core loss characteristics of Fe-based amorphous alloys, Intermetallics 17 (2009) 278–280.
[3] N. Zhang, Z. Hu, B. Shen, G. He, Y. Zheng, An integrated source-grid-load planning model at the macro level: case study for China's power sector, Energy 126 (2017) 231–246.
[4] J. Xu, Y. Yang, W. Li, Z. Xie, X. Chen, Effect of Si addition on crystallization behavior, thermal ability and magnetic properties in high Fe content Fe-Si-B-P-Cu-C alloy, Mater. Res. Bull. 97 (2018) 452–456.
[5] H. Zheng, L. Hu, X. Zhao, C. Wang, Q. Sun, T. Wang, X. Hui, Y. Yue, X. Bian, Poor glass-forming ability of Fe-based alloys: its origin in high-temperature melt dynamics, J. Non-Cryst. Solids 471 (2017) 120–127.
[6] O. Gutfleisch, M.A. Willard, E. Bruck, C.H. Chen, S.G. Sankar, J.P. Liu, Magnetic materials and devices for the 21st century: stronger, lighter, and more energy efficient, Adv. Mater. 23 (2011) 821–842.
[7] Y. Ogawa, M. Naoe, Y. Yoshizawa, R. Hasegaw, Magnetic properties of high Bs Fe-based amorphous material, J. Magn. Magn. Mater. 304 (2006) E675–E677.
[8] F. Wang, A. Inoue, Y. Han, S.L. Zhu, F.L. Kong, E. Zanaeva, G.D. Liu, E. Shalaan, F. Al-Marzouki, A. Obaid, Soft magnetic Fe-Co-based amorphous alloys with extremely high saturation magnetization exceeding 1.9 T and low coercivity of 2 A/m, J. Alloy. Compd. 723 (2017) 376–384.
[9] H. Zhang, X. Tang, R. Wei, S. Zhu, J. Yang, W. Song, J. Dai, X. Zhu, Y. Sun, Microstructure refinement and magnetization improvement in CoFe thin films by high magnetic field annealing, J. Alloy. Compd. 729 (2017) 730–734.
[10] P. Chen, A. Wang, C. Zhao, A. He, G. Wang, C. Chang, X. Wang, C.-T. Liu, Development of soft magnetic amorphous alloys with distinctly high Fe content, Science China Physics, Mech. Astron. 60 (2017).
[11] V. Zhukova, O.A. Korchuganova, A.A. Aleev, V.V. Tcherdyntsev, M. Churyukanova, E.V. Medvedeva, S. Seils, J. Wagner, M. Ipatov, J.M. Blanco, S.D. Kaloshkin, A. Aronin, G. Abrosimova, N. Orlova, A. Zhukov, Effect of annealing on magnetic properties and structure of Fe-Ni based magnetic microwires, J. Magn. Magn. Mater. 433 (2017) 278–284.
[12] K. Suzuki, G. Herzer, Magnetic-field-induced anisotropies and exchange softening in Fe-rich nanocrystalline soft magnetic alloys, Scr. Mater. 67 (2012) 548–553.
[13] C. Zhao, A. Wang, S. Yue, T. Liu, A. He, C. Chang, X. Wang, C.-T. Liu, Significant improvement of soft magnetic properties for Fe(Co)BPSiC amorphous alloys by magnetic field annealing, J. Alloy Compd. 742 (2018) 220–225.
[14] S. Wen, Y. Ma, D. Wang, Z. Xu, S. Awaji, K. Watanabe, Magnetostriction enhancement by high magnetic field annealing in cast $Fe_{81}Ga_{19}$ alloy, J. Magn. Magn. Mater. 442 (2017) 128–135.
[15] R. Madugundo, O. Geoffroy, T. Waeckerle, B. Frincu, S. Kodjikian, S. Rivoirard, Improved soft magnetic properties in nanocrystalline FeCuNbSiB Nanophy ® cores by intense magnetic field annealing, J. Magn. Magn. Mater. 422 (2017) 475–478.
[16] X. Li, J. Liu, C. Qu, K. Song, L. Hu, L. Wang, Preparation and properties of FeBP Sn soft magnetic amorphous alloys with Fe contents higher than 83%, J. Non-Cryst. Solids 469 (2017) 27–30.
[17] P. Chen, T. Liu, F. Kong, A. Wang, C. Yu, G. Wang, C. Chang, X. Wang, Ferromagnetic element microalloying and clustering effects in high B_s Fe-based amorphous alloys, J. Mater. Sci. Technol. (2017).
[18] F. Chen, T. Zhang, J. Wang, L. Zhang, G. Zhou, Investigation of domain wall pinning effect induced by annealing stress in sintered Nd–Fe–B magnet, J. Alloy. Compd. 640 (2015) 371–375.
[19] C. Zhao, A. Wang, A. He, S. Yue, C. Chang, X. Wang, R.-W. Li, Correlation between soft-magnetic properties and T_{x1}-T_c in high B_s FeCoSiBPC amorphous alloys, J. Alloy. Compd. 659 (2016) 193–197.
[20] J.S. Blázquez, J. Marcin, F. Andrejka, V. Franco, A. Conde, I. Skorvanek, Anisotropy field distribution in soft magnetic Hitperm alloys submitted to different field annealing processes, J. Alloy. Compd. 658 (2016) 367–371.
[21] Z. Li, Y. Dong, S. Pauly, C. Chang, R. Wei, F. Li, X.-M. Wang, Enhanced soft magnetic properties of Fe-based amorphous powder cores by longitude magnetic field annealing, J. Alloy. Compd. 706 (2017) 1–6.
[22] E.A. Périgo, S. Nakahara, Y. Pittini-Yamada, Y. de Hazan, T. Graule, Magnetic properties of soft magnetic composites prepared with crystalline and amorphous powders, J. Magn. Magn. Mater. 323 (2011) 1938–1944.
[23] A.D. Wang, H. Men, B.L. Shen, G.Q. Xie, A. Makino, A. Inoue, Effect of P on crystallization behavior and soft-magnetic properties of $Fe_{83.3}Si_4Cu_{0.7}B_{12-x}P_x$ nanocrystalline soft-magnetic alloys, Thin Solid Films 519 (2011) 8283–8286.

[24] J. Fornell, S. González, E. Rossinyol, S. Suriñach, M.D. Baró, D.V. Louzguine-Luzgin, J.H. Perepezko, J. Sort, A. Inoue, Enhanced mechanical properties due to structural changes induced by devitrification in Fe–Co–B–Si–Nb bulk metallic glass, Acta Mater. 58 (2010) 6256–6266.
[25] C. Fan, C.T. Liu, G. Chen, P.K. Liaw, Quantitatively defining free-volume, interconnecting-zone and cluster in metallic glasses, Intermetallics 57 (2015) 98–100.
[26] D.V. Gunderov, E.V. Boltynjuk, E.V. Ubyivovk, A.V. Lukyanov, A.A. Churakova, A.R. Kilmametov, Y.S. Zamula, R.Z. Valiev, Cluster structure in amorphous Ti-Ni-Cu alloys subjected to high-pressure torsion deformation, J. Alloy. Compd. 749 (2018) 612–619.
[27] B. Zang, R. Parsons, K. Onodera, H. Kishimoto, A. Kato, A.C.Y. Liu, K. Suzuki, Effect of heating rate during primary crystallization on soft magnetic properties of melt-spun Fe-B alloys, Scr. Mater. 132 (2017) 68–72.
[28] Augusto Visintin, A Weiss-type model of ferromagnetism, Phys. B 275 (2000) 87–91.
[29] M. Soderžnik, H. Sepehri-Amin, T.T. Sasaki, T. Ohkubo, Y. Takada, T. Sato, Y. Kaneko, A. Kato, T. Schrefl, K. Hono, Magnetization reversal of exchange-coupled and exchange-decoupled Nd-Fe-B magnets observed by magneto-optical Kerr effect microscopy, Acta Mater. 135 (2017) 68–76.
[30] S. Kaloshkin, M. Churyukanova, V. Zadorozhnyi, I. Shchetinin, R.K. Roy, Curie temperature behaviour at relaxation and nanocrystallization of Finemet alloys, J. Alloy. Compd. 509 (2011) S400–S403.
[31] A. Gavrilović, L.D. Rafailović, D.M. Minić, J. Wosik, P. Angerer, D.M. Minić, Influence of thermal treatment on structure development and mechanical properties of amorphous $Fe_{73.5}Cu_1Nb_3Si_{15.5}B_7$ ribbon, J. Alloy. Compd. 509 (2011) S119–S122.
[32] A.M. Severino, A.D. Santos, E.P. Missell, Changes in induced anisotropy and magnetostriction in co-based amorphous-alloys, J. Magn. Magn. Mater. 96 (1991) 167–174.
[33] C. Miguel, A.P. Zhukov, J.J. del Val, A.R. de Arellano, J. Gonzalez, Effect of stress and/or field annealing on the magnetic behavior of the (Co77Si13.5B9.5)(90) Fe7Nb3 amorphous alloy, J. Appl. Phys. 97 (2005) 8.
[34] K.Y. Ho, F. Xu, X.Y. Xiong, Effects of magnetic and stress annealing on the change in magnetostriction for magnetically soft amorphous-alloys, J. Magn. Magn. Mater. 119 (1993) 318–320.